

PAPER • OPEN ACCESS

Wire bonded 3D coils render air core microtransformers competitive

To cite this article: A Moazenzadeh *et al* 2013 *J. Micromech. Microeng.* **23** 114020

View the [article online](#) for updates and enhancements.

You may also like

- [A fully MEMS-compatible process for 3D high aspect ratio micro coils obtained with an automatic wire bonder](#)
K Kratt, V Badilita, T Burger et al.
- [Development and Optimization of Thin-Film Technology Based Micro Inductors and Transformers](#)
Sebastian Beringer, Dragan Dinulovic, Martin Haug et al.
- [Fully Integrated Spiral-type Microtransformers on a Silicon Substrate](#)
Jae Y. Park and Jong U. Bu

Wire bonded 3D coils render air core microtransformers competitive

A Moazenadeh¹, N Spengler^{1,2}, R Lausecker¹, A Rezvani³, M Mayer³, J G Korvink^{2,4} and U Wallrabe¹

¹ Laboratory for Microactuators, Department of Microsystems Engineering (IMTEK), University of Freiburg, Georges-Koehler-Allee 102, D-79110 Freiburg, Germany

² Freiburg Institute for Advanced Studies (FRIAS), University of Freiburg, Albertstrasse 19, D-79104 Freiburg, Germany

³ Department of Mechanical and Mechatronics Engineering, University of Waterloo, 200 University Ave. W., Waterloo, Canada

⁴ Simulation Laboratory, Department of Microsystems Engineering (IMTEK), University of Freiburg, Georges-Koehler-Allee 102, D-79110 Freiburg, Germany

E-mail: wallrabe@imtek.uni-freiburg.de

Received 25 March 2013, in final form 11 September 2013

Published 25 October 2013

Online at stacks.iop.org/JMM/23/114020

Abstract


We present a novel wafer-level fabrication method for 3D solenoidal microtransformers using an automatic wire bonder for chip-scale, very high frequency regime applications. Using standard microelectromechanical systems fabrication processes for the manufacturing of supporting structures, together with ultra-fast wire bonding for the fabrication of solenoids, enables the flexible and repeatable fabrication, at high throughput, of high performance air core microtransformers. The primary and secondary solenoids are wound one on top of the other in the lateral direction, using a 25 μm thick insulated wire. Besides commonly available gold wire, we also introduce insulated copper wire to our coil winding process. The influence of copper on the transformer properties is explored and compared to gold. A simulation model based on the solenoids' wire bonding trajectories has been defined using the FastHenry software to accurately predict and optimize the transformer's inductive properties. The transformer chips are encapsulated in polydimethylsiloxane in order to protect the coils from environmental influences and mechanical damage. Meanwhile, the effect of the increase in the internal capacitance of the chips as a result of the encapsulation is analyzed. A fabricated transformer with 20 windings in both the primary and the secondary coils, and a footprint of 1 mm^2 , yields an inductance of 490 nH, a maximum efficiency of 68%, and a coupling factor of 94%. The repeatability of the coil winding process was investigated by comparing the data of 25 identically processed devices. Finally, the microtransformers are benchmarked to underline the potential of the technology in rendering air core transformers competitive.

(Some figures may appear in colour only in the online journal)

1. Introduction

Many new handheld electronic devices are introduced and fabricated each year. Although they are different in their

functionality and applications, many of them have a battery as their primary energy source. Since batteries provide constant voltage levels, the necessity of power converters to accommodate the requirements of different electronic function blocks become obvious. Since almost all of the energy which is used by a function block needs to pass through a power converter, the converter should be as efficient as possible. Furthermore, the trend towards the further miniaturization of

 Content from this work may be used under the terms of the [Creative Commons Attribution 3.0 licence](http://creativecommons.org/licenses/by/3.0/). Any further distribution of this work must maintain attribution to the author(s) and the title of the work, journal citation and DOI.

electronic devices makes the integration and miniaturization of power convertors indispensable.

Among the electronic components of power conversion circuits, transformers are the preferred candidates for miniaturization since they occupy the largest relative volume. In conventional electronics transformers are standard passive elements based on well-established fabrication methods, providing a high efficiency when compared with most other circuit elements. In the micro world, transformers are increasingly playing an important role as essential subunits of power-converters [1] and isolator circuits [2]. Microtransformers have been studied and fabricated for more than two decades, however, there is still much space for improvement in terms of performance and ease of microfabrication. Miniaturization and integration, while maintaining high electrical performance, are the two key challenges that developers face. One way to enhance transformer performance, whilst maintaining the same footprint, is the co-integration of a magnetic core, but besides the additional complexities in material processing and patterning, material losses limit magnetic-core performance in and above the MHz regime [3]. Increasing the switching frequency in the convertor offers another route which leads to further reduction in size of the inductors [4]. However, this approach introduces additional high frequency-related parasitic losses, via the skin or proximity effect [5].

An optimized fabrication strategy for the inductive elements offers further miniaturization potential for the transformers. Compact primary and secondary coils, with high quality and coupling factors in the very high frequency (VHF) regime, can result in a transformer with reasonable efficiency, without the need to further increase frequency or add a magnetic core.

A planar 2D layout is the common choice for the transformers' coils. These are available in two versions, either spiral planar coils [6–10] or stacked planar coils [11, 12]. These inductors are typically fabricated by electroplating metal layers with thicknesses of several microns on top of an insulating substrate. An advantage of flat transformers is their compatibility with a straightforward, microelectromechanical systems (MEMS)-compatible fabrication process. This advantage is paid for by a relatively low quality factor [13] and a large footprint.

3D solenoids with different cross-sections, such as rectangular or circular shapes, mostly with the coil axis parallel to the substrate, have been used as inductors in microtransformers [1, 14–17]. Besides higher inductance density, 3D inductors provide more concentrated and uniform magnetic fields [13], which lead to stronger coupling between the coils when compared to a 2D design. On the other hand, these solenoids are mostly fabricated in a manner similar to the 2D coils, i.e., by multilevel metal electroplating and mold lithography, which makes their fabrication procedures even more complex and time consuming. The limitation in winding density is another drawback of this coil's design.

The fabrication of 3D micro coils with their axis perpendicular to the substrate using an automatic wire bonder

was initially reported by Kratt *et al* [18]. In [2], Raimann *et al* applied the technique to fabricate microtransformers on magnetic cores. The cores were cast in glass rods, using a thermoplastic filled with ferrite nanoparticles, and were manually assembled onto a PCB for coil winding. In [19], we improved the technology towards a complimentary metal–oxide–semiconductor (CMOS) compatible, slim batch fabrication, by completely avoiding magnetic materials and simply using SU-8 polymer cores instead, which behave like air from a magnetic point of view, and without compromising performance.

Wire bonding is an established, state-of-the-art CMOS-compatible assembly and packaging technique. Although it is a serial process, it provides high throughput and is therefore widely used in industrial applications. Wire bonders allow the highly precise shaping of micron-sized wires at high speed. They are capable of shaping 3D inductors with various cross-sections, due to the circular or rectangular supporting posts or magnetic cores [19, 20]. When compared to the successive electroplating of metal, the method is faster, and the metal's quality, i.e., its mechanical properties, its purity, and its reduced number of voids, is better. Wire bonding is straightforwardly incorporated into existing fabrication chains, allowing direct on-chip integration into a given circuit. The process is highly flexible for numerous applications, because wires of diverse materials, such as copper, gold, aluminum or platinum are available in various diameters, with or without insulation layer.

The required winding trajectories, for both the primary and the secondary coils, are defined in an in-house developed code based on the MATLAB[®] software. Details of the coil geometry, such as the slope or pitch of the windings, are all considered in this code. Without the need for new photolithography masks, a variation in coil design is achieved simply by modifying the trajectory of capillary that shapes the wire. Also, the number of windings can be varied from coil to coil in a similar manner. The geometry of the generated trajectory may also serve as input data for a FastHenry simulation model. The FastHenry software package computes the frequency-dependent self and mutual inductance, as well as the electrical resistance, of 3D conductive structures [21]. The transformer properties can hence be predicted and optimized prior to fabrication.

In this paper, we report on the simulation and fabrication results for an improved version of the SU-8 core transformers with higher performance compared to [19]. Transformers with magnetic cores typically operate in the kHz to low MHz regime, due to self-resonance saturation and magnetic-core internal losses. On the other hand, 2D air core radio frequency (RF) transformers show resonance at GHz frequencies, does not offer enough inductance density which is needed for the power conversion in MHz regime applications [11, 22]. The focus of this work is to bridge the gap in between, by introducing a device with high performance in all aspects at VHF (30–300 MHz) regime by applying fast, precise, repeatable and flexible fabrication process.

In section 3.1 we describe the simulation and measurement results for transformers based on gold wire. In

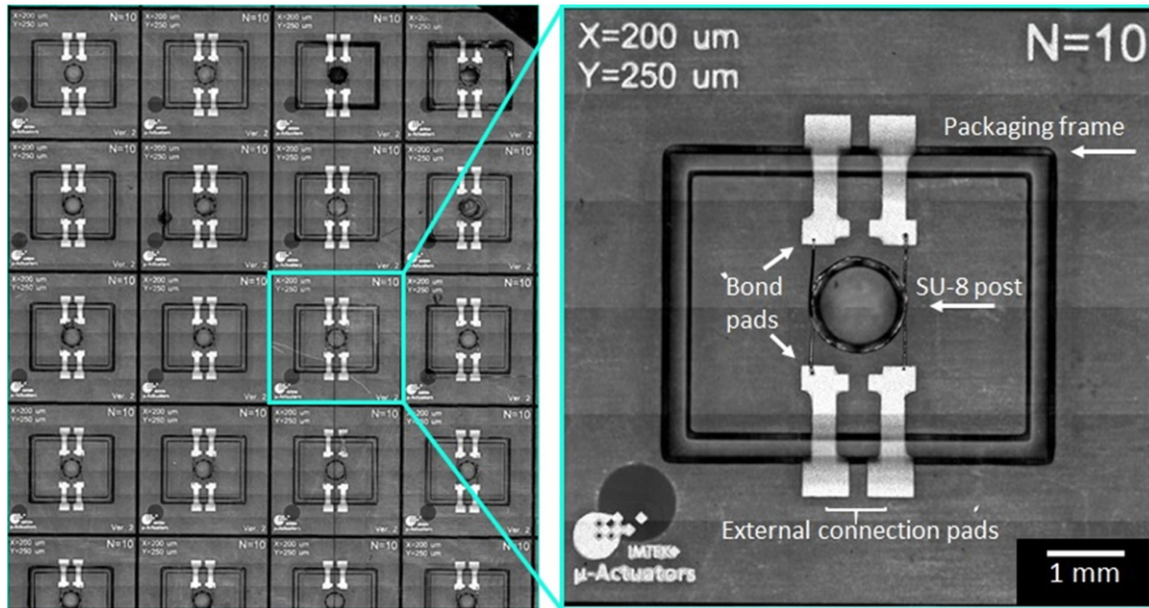


Figure 1. *Left:* photograph of a quarter of wafer, showing array of wire bonded chips. *Right:* top view of a transformer chip. The SU-8 post located at a center of the chip with diameter of 1.15 mm and high of 650 μm . Pads and traces are made by 12 μm electroplating gold on a borosilicate substrate.

section 3.2 we present for the first time a transformer with wire bonded copper coils, and compare the results with those from gold wire transformers. In section 3.3 we analyze the influence of the polydimethylsiloxane (PDMS) package on the electrical properties of the chips. The repeatability of the process is further investigated in section 3.4, verifying the eligibility of the process for batch fabrication.

2. Design and fabrication

A 3D solenoidal design was chosen for both the primary and the secondary coil of the transformer due to the advantages when compared to 2D planar coil geometries. Both solenoids were wound symmetrically, starting from the same height above the substrate. One coil is wound on top of the other in the lateral direction, to ensure a maximum coupling between the inner primary and the outer secondary coils. The solenoids' coincident axes are oriented perpendicular to the substrate, which enabled us to straightforwardly vary the number of windings without the need to change the footprint size. It also allowed us to access the inner part of the solenoids to integrate a magnetic core or a cooling element, if necessary.

The solenoids occupy 1 mm^2 of substrate area and are 500 μm high. The primary–secondary winding ratio is 1:1 for all prototypes. Using a 25 μm thick insulated wire (X-Wire™, Microbonds, Canada) provided enough cross-section and circumference to achieve a low resistance in the low and high frequency regimes. In addition, having initial insulation (a polymer with 100 nm thickness), there was no need for extra processing to achieve wire passivation. The circular cross-section of the wire provided a more homogenous current distribution when compared to a lithographically patterned rectangular conductor, resulting in less internal loss at high frequency. In order to connect the wire ends to the substrate, gold bond pads were electroplated, each with an area of

0.180 mm^2 and a thickness of 12 μm . The bond pads were connected to a second set of pads for external connection by traces of 900 μm length, a width of 300 μm and a thickness of 12 μm . The external pads have an area of 0.300 mm^2 and thickness of 12 μm . A photograph of a quarter of wafer, showing array of wire bonded chips and a top view of the transformer chip are shown in figure 1.

The inductance of small solenoids exhibits a quadratic dependency on the number of windings [23], however, this is to be contrasted with a linear dependency of the electrical resistance on the winding number. Therefore, by modeling with FastHenry, the optimum number of windings needed to obtain maximum quality- and coupling factors for the transformers has been verified. Depending on the solenoid's starting and total height, wire thickness and pitch, up to 20 windings can be placed in one layer for each solenoid. The simulation results show a constant increase in both coupling- and quality factor by increasing the number of turns in a range of 4 to 20 (figures 2 and 3).

The fabrication started with a 4-inch borosilicate substrate. Borosilicate wafers were chosen to avoid the induction of eddy currents in the substrate and hence to minimize substrate-related losses. After evaporating a 15 nm/150 nm Cr/Au seed layer, a 20 μm thick mold for pads and traces was patterned using the AZ-9260 photoresist. Then, 12 μm of gold was electroplated to fully cover the RF conductive skin depth, and hence to minimize the electrical resistance of the bond pads, external pads, and traces (figure 5(a)). After stripping the mold and etching the seed layer, a thick SU-8 process was employed to define an array of high cylindrical posts, which were used as supporting structures during the wire bonding of the solenoids. Each post had a diameter of 1.15 mm and was 650 μm high. For the final encapsulation, an SU-8 frame was patterned during the same photolithographic step to be later filled with PDMS as

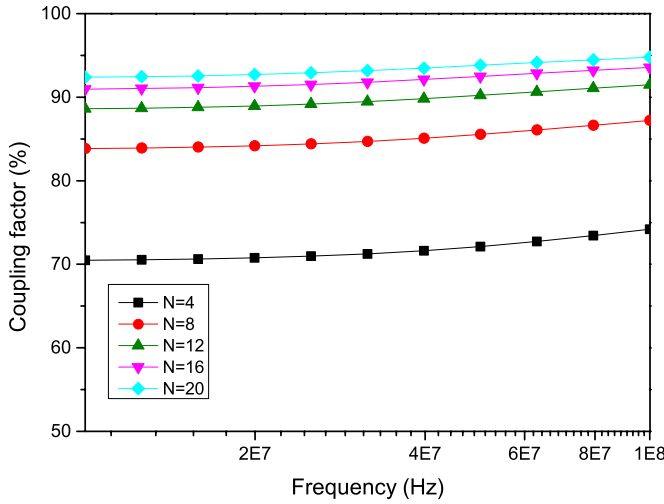


Figure 2. Simulated dependency of the coupling factor on the frequency for a diverse number of windings.

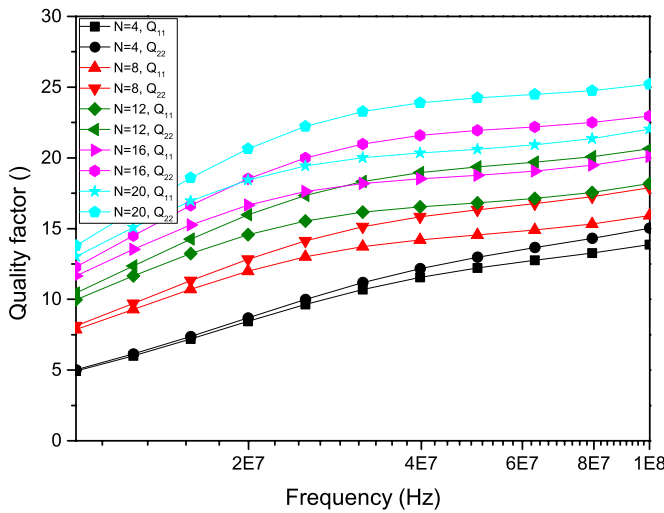


Figure 3. Simulated dependency of the quality factor on the frequency for a diverse number of windings.

an encapsulation material (figure 5(b)). Details of the SU-8 process were already reported in [18].

After a short O₂-plasma cleaning step for 2 min at 40 °C, 0.3 mbar and a power of 1000 W at 2.54 GHz, a modified, automated ball-wedge wirebonder (ESEC WB 3100^{plus}, ESEC, Switzerland) was employed to wind two solenoids, each with 20 windings, in a helical trajectory around the posts. The starting height of the coils was set to 50 μm above the surface of the substrate to achieve coils with a nominal height of 500 μm for 20 windings. Thus, a distance of 100 μm is left between the upper edge of the post and the upper winding serving as a safety margin. This space is enough in order to fixate the wire on the post and to prevent the final winding from jumping off the post. The winding time for each transformer was only 16 s (figure 5(c)).

The coils themselves are already stable, however, to provide a physical protection for both the coils and their bond connections as well as to make the chip handling easier, Sylgard[®] 184 PDMS was then statically dispensed into the SU-8 frame at a temperature of 80 °C, which was subsequently

cured at 70 °C for 2 h in an oven to form the package (figure 5(d)). A cross-section view of the fully processed transformer chip, as well as a schematic of the fabrication process flow and an overview picture of a chip, are shown in figures 4 and 5.

3. Characterization and results

The high frequency characterization of the transformers was performed using a 2-port, on-wafer measurement method. The scattering parameters of the transformers were measured using an Agilent E5071A vector network analyzer which was connected to a Cascade Microtech 9000 probe-station, equipped with two SG/GS-500 microprobes. Prior to the measurement, open, short, load and through calibrations were done using an impedance standard substrate (ISS). The scattering parameters of the transformers were recorded simultaneously as a function of a logarithmic frequency sweep from 1 MHz up to 1 GHz. The power efficiency of the transformers, the output load power versus the transformer input power, was computed directly from the scattering parameters by equation (1) [24]:

$$\eta_{z_0} = \frac{|S_{21}|^2}{1 - |S_{11}|^2} \quad (1)$$

with $Z_0 = 50 \Omega$ as a nominal impedance of the network analyzer which served as a load impedance of the measurements. The maximum transducer power gain given by equation (2) occurs when the source and load are conjugately matched to the transformer [24]:

$$G_{T_{max}} = \frac{|S_{21}|}{|S_{12}|} (K - \sqrt{K^2 - 1}) \quad (2)$$

With K , the Rollet stability condition defined as:

$$K = \frac{1 - |S_{11}|^2 - |S_{22}|^2 + |S_{11}S_{22} - S_{12}S_{21}|^2}{2|S_{12}S_{21}|} \quad (3)$$

By converting the S -parameters to Z -parameter data, and extracting the real and imaginary parts of the impedance for each port at each frequency, the inductance, electrical resistance and quality factor, as well as the coupling factor of the transformers were determined by using equations (4):

$$\begin{aligned} L_{xy} &= \frac{\Im[Z_{xy}]}{2\pi f} \\ R_{xy} &= \Re[Z_{xy}] \\ Q_{xy} &= \frac{\Im[Z_{xy}]}{\Re[Z_{xy}]} \\ k &= \sqrt{\frac{\Im[Z_{12}]\Im[Z_{21}]}{\Im[Z_{11}]\Im[Z_{22}]}} \end{aligned} \quad (4)$$

where x and y denote the port numbers. This set of formulae was also used for analyzing the output data of the FastHenry model.

3.1. Transformers with gold wire

The present section discusses the simulation and measurement results of a gold wire transformer. The next section presents the corresponding results achieved with copper wire transformers.

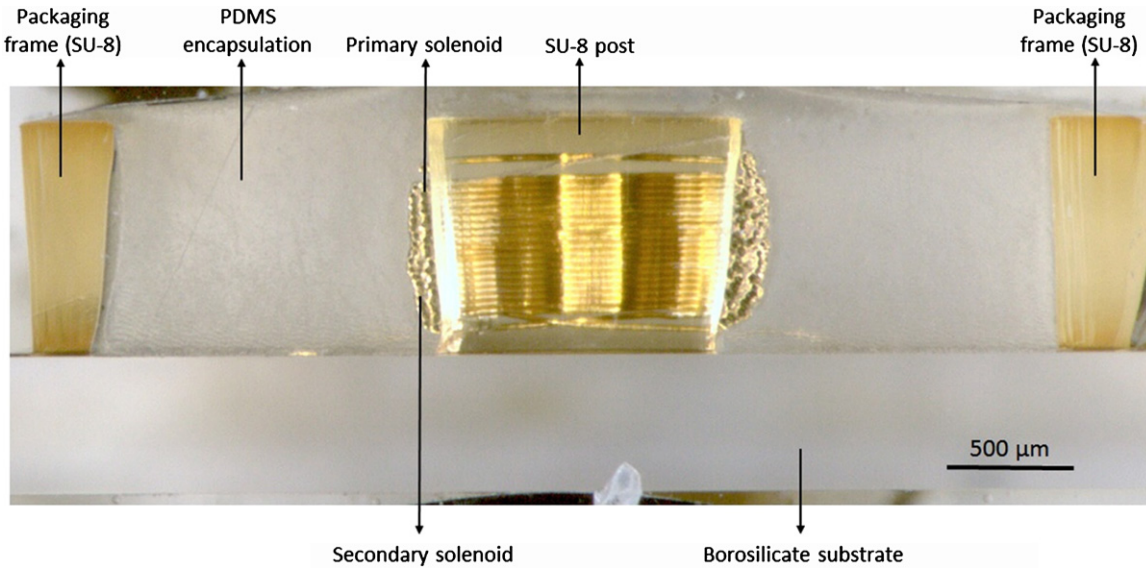


Figure 4. Polished cross-section image of the transformer chip. One coil is wound on top of the other in the lateral direction to ensure a maximum of magnetic coupling between the inner primary and the outer secondary coils.

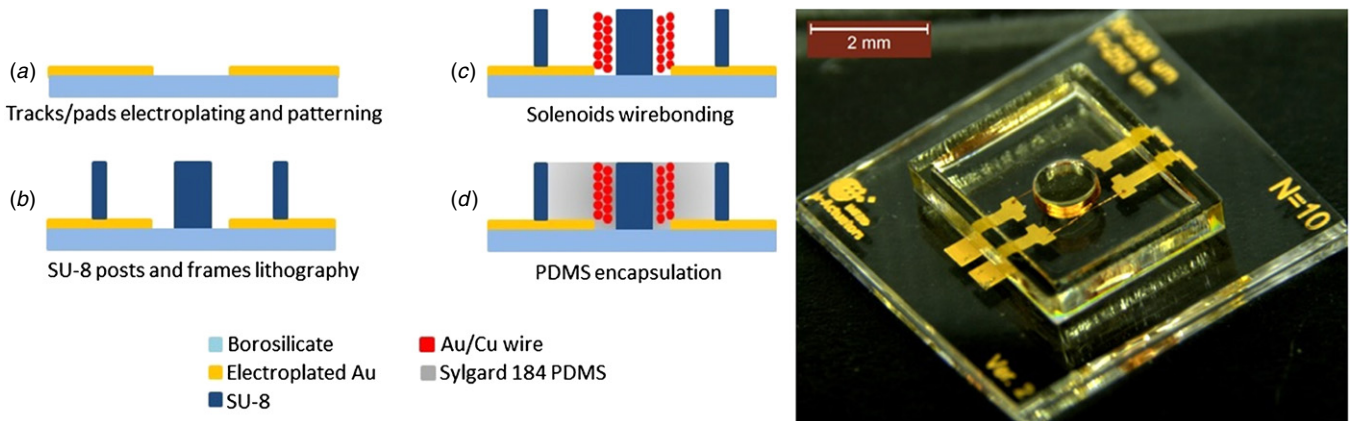


Figure 5. Left: wire-bonded microtransformer manufacturing process flow (a)–(d). Right: a complete copper wire-bonded transformer chip, encapsulated in PDMS.

Table 1. Gold wire transformer measurement and simulation results.

	L_{11} (nH)	L_{22} (nH)	R_{11} (Ω)	R_{22} (Ω)	Q_{11max}	Q_{22max}	k (%)	η_{max} (%)
f (MHz)	1	1	1	1	72	78	<236	54
Measurement	482	464	3.76	3.65	18	27	94	67
Simulation	539	507	3.03	2.91	20	24	94	–

The self-resonance frequency of the transformer was found to be 236 MHz. Far below the self-resonance frequency, we measured the primary and the secondary solenoids' self-inductances to be $L_{11} = 482$ nH and $L_{22} = 464$ nH. The mutual-inductances were measured to be $L_{12} = L_{21} = 445$ nH, as is also shown in figure 6(a). The 2-port resistance of the transformer is illustrated in figure 6(b). The resistance of the primary coil was 3.76 Ω , and of the secondary coil 3.65 Ω , both measured at a frequency of 1 MHz. For both solenoids the resistance increased with increasing frequency due to the skin- and proximity effects. The quality factor of the primary solenoid reached a maximum value of 18, whereas it was 27 in

the secondary solenoid (figure 6(c)). This difference resulted from the difference in the primary and the secondary solenoid's winding trajectories and diameters. The coupling factor had a constant value of 94% over the whole frequency range below the self-resonance frequency. The efficiency of the transformer reached a maximum value of 67% at a frequency of 54 MHz for the 50 Ω load provided by the network analyzer (figure 6(d)). Table 1 summarizes the main measurement results of the gold transformer.

The simulation results obtained by FastHenry are also given in table 1. Due to the fact that FastHenry does not consider capacitance effects, the values for the inductance

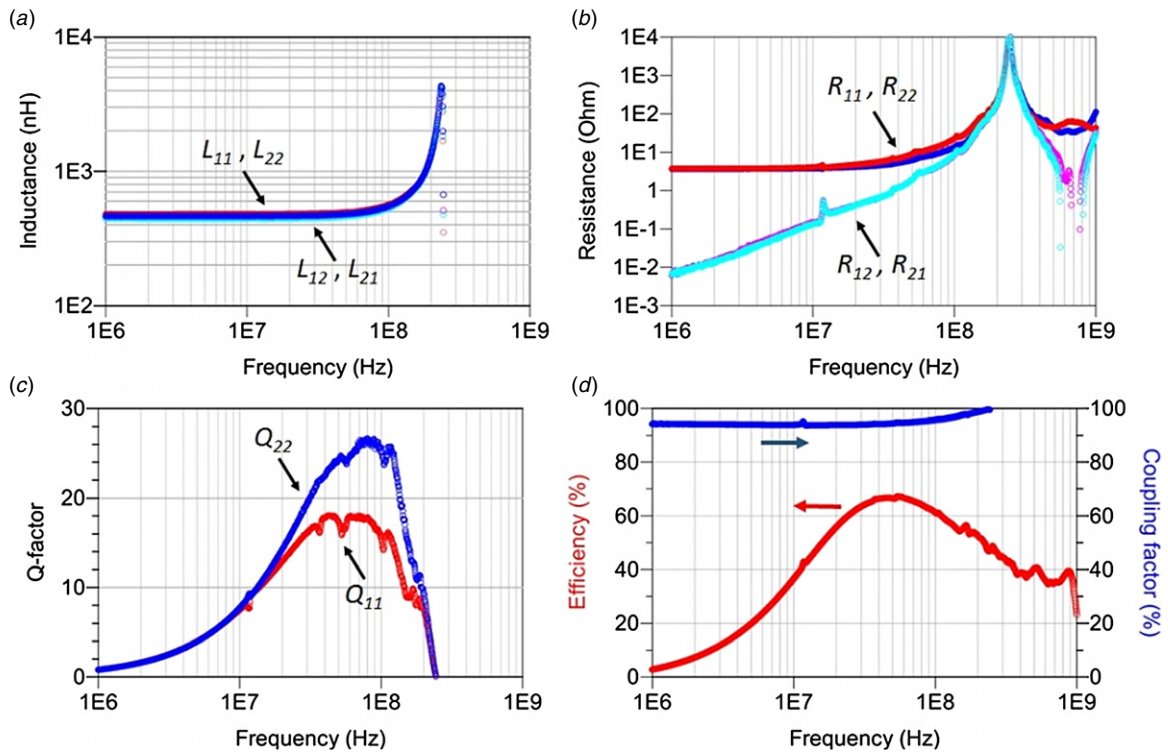


Figure 6. Gold wire transformer 2-port measurement results.

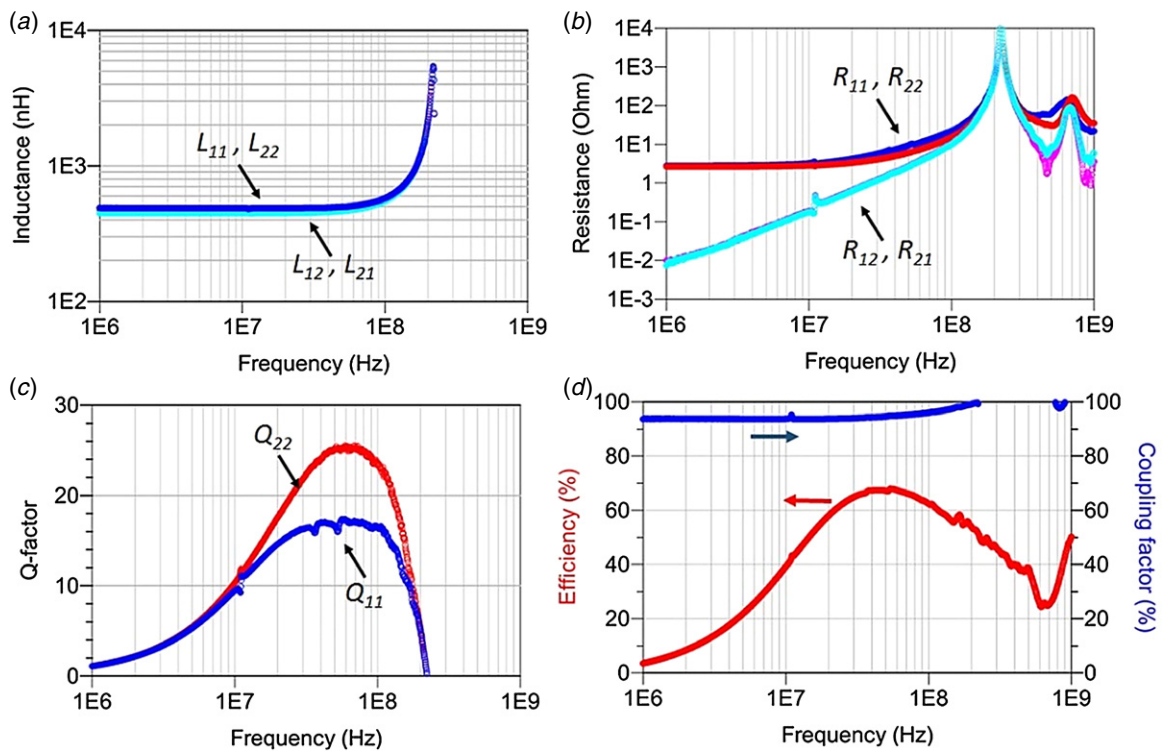


Figure 7. Copper wire transformer 2-port measurement results.

and consequently for the quality factor are not valid around the self-resonance, however, below the resonance frequency the predicted values are acceptable. A comparison of the simulation and measurement results for the inductances and coupling factor shows a deviation of less than 10%, however, this difference is increased for the case of

the resistance. The reason is due to the fact that the pads, the traces and contact resistance, have not been considered in the model, and that FastHenry can only simulate conductors with rectangular cross-section, whereas in our case the wire conductors have a circular cross-section.

Table 2. Benefits and challenges of using copper as a coil material from the wire bonding manufacturing and applications point of view [25, 26].

Advantages	Disadvantages
<ul style="list-style-type: none"> • Better electrical conductivity in the DC regime • Better thermal properties • Lower cost • Higher stiffness 	<ul style="list-style-type: none"> • Necessity of coating wire to prevent oxidation • Need of inert forming gas during wire bonding • Chance of under-pad damage due to wire stiffness • Lower skin depth for high frequency applications

Table 3. Copper wire transformer measurement and simulation results.

	L_{11} (nH)	L_{22} (nH)	R_{11} (Ω)	R_{22} (Ω)	$Q_{1\max}$	$Q_{2\max}$	k (%)	η_{\max} (%)
f (MHz)	1	1	1	1	77	68	<218	54
Measurement	490	468	2.79	2.64	17	25	94	68
Simulation	539	507	2.15	2.06	20	25	94	–

3.2. Transformer with copper wire

Currently, gold is the most popular wire bond material due its good adhesion to bond pads (mainly Au and Al). Recently, copper wire has attracted more attention as an alternative wire candidate to replace gold. When compared to gold, copper is $\sim 25\%$ more conductive in the DC regime, it has better thermal properties, it has higher mechanical stiffness, and it is also less expensive than gold, which results in lower fabrication costs and better all-round performance [25, 26].

Despite the mentioned benefits, copper wire bonding has its own challenges too. For example, the rapid oxidation of copper wire in air can degrade its bonding ability within a few days. This necessitates a coating of the copper wire with different materials such as Pd, Ag or a polymer, and also requires protection of the ball melt with forming gas. In addition, due to the increased hardness of copper wire, die damage during copper wire bonding is more likely [26]. Finally, especially for high frequency applications, copper has a lower skin depth which results in higher frequency-dependent resistivity values at a particular frequency, when compared to gold.

The benefits and disadvantageous of using copper wire for coil manufacturing using wire bonding are summarized in the table 2.

Also the parameters of the copper wire bonding process needed to be carefully adjusted to achieve reliable bonds. The heater plate temperature of the wire bonder was set to 150 °C which is 25 °C higher than for the gold wire bonding. The copper ball bond process required 15% higher ultrasonic power, 100 mN higher impact force, 50 mN higher bond force, 10 ms longer bond time and 35% higher pre-ultrasonic power compared to the gold ball bonding. The bonding parameters for the wedge bonding were almost similar for the copper and gold wire bonding. However, an additional cleaning step ‘scrub’ was needed to remove the insulation layer and to form a proper wedge connection for the insulated wires in general. In order to prevent the copper wire from oxidation during the ball bond formation, the constant flow rate of the pure nitrogen as a shielding gas was set to 47 l min⁻¹.

The self-resonance frequency of the transformer was found to be 218 MHz. Far below the self-resonance frequency we measured the primary and the secondary solenoids’ self-inductances to be $L_{11} = 490$ nH and $L_{22} = 468$ nH. The

mutual-inductances were measured to be $L_{12} = L_{21} = 449$ nH as shown in figure 7(a). The 2-port resistance behavior of the transformer is illustrated in figure 7(b), with the resistance of the primary coil 2.79 Ω and the secondary coil 2.64 Ω when measured at 1 MHz. When compared to the gold wire bonded transformer, the resistance was found to be around 1 Ω less for each port at the same frequency, resulting from the higher electrical conductivity. However, by increasing the frequency, the skin depth and proximity effects became dominant, which affected the electrical resistance and resulted in almost the same electrical behavior of the gold and copper conductors over the high frequency regime.

The quality factor of the primary solenoid attained a maximum value of 17, the secondary coil achieved a quality factor of 25 (figure 7(c)). The coupling factor was constantly 94% for frequencies below the self-resonance. The efficiency reached its maximum value of 68% at a frequency of 54 MHz for a network analyzer load of 50 Ω , as shown in figure 7(d). Table 3 summarizes the measurement and simulation results of the copper transformer.

3.3. Analysis of PDMS packaging effects

The most delicate part of the chip is the wedge bond. A practical solution for the wedge bond protection is to bond a ball bump (security bump) on top of it. However, since our specific wire bonder can produce ball bumps only as part of a full loop process (similar to ball-stitch process), the bonding direction is not controllable by the coil winding code, and the security bump is not applicable.

The encapsulation of a microtransformer chip provides a practical solution in order to protect the delicate bonds and wiring from external mechanical damage. Meanwhile it makes the chip handling easier, especially for the further processes like assembling it into the target circuit. However, replacing air ($\epsilon_r = 1$) with a dielectric material ($\epsilon_r > 1$) in an inductor-based system, results in an increase of capacitance and a change in the electrical behavior.

In this paper, Sylgard[®] 184 PDMS is used as the encapsulation material. Besides its low volume shrinkage, Sylgard[®] 184 has a dielectric constant of only 2.65, which is lower than most epoxies and other silicone materials [27, 28]. To investigate the effect of encapsulation on the electrical

Table 4. Measured values of seven identical transformer chips, before and after the PDMS encapsulation. Only the resonance frequency showed a drastic change.

	L (nH)	Q_{\max}	η_{\max} (%)	Resonance
Before packaging	404 ± 4	23.40 ± 0.5	63.59 ± 2.39	–
@ f (MHz)	1	85	61	312 ± 3
After packaging	406 ± 5	23.33 ± 1.21	64.03 ± 2.31	–
@ f (MHz)	1	84	60	258 ± 2

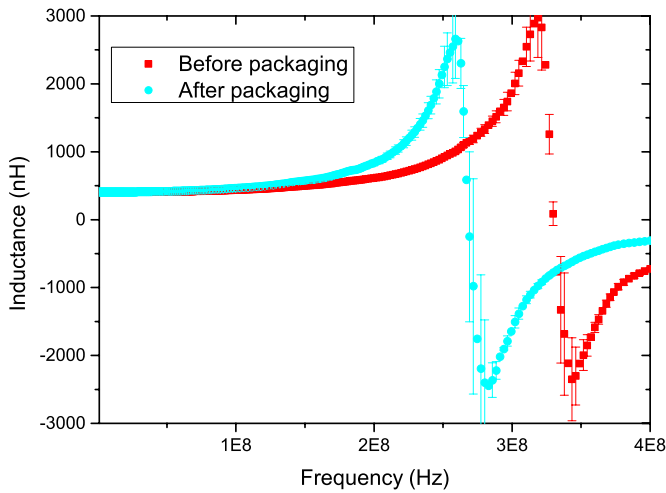


Figure 8. Measured inductance versus frequency of the primary solenoid of seven identical transformer chips before and after encapsulation with PDMS. The resonance frequency was decreased by 21% after encapsulation.

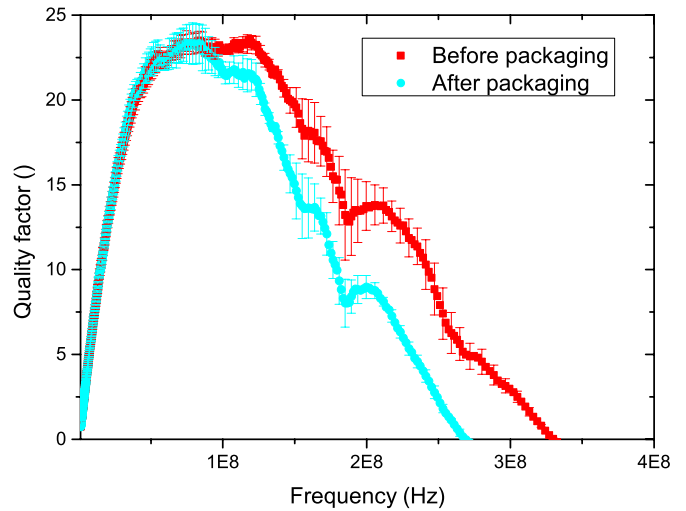


Figure 9. Measured Q -factor versus frequency of the primary solenoid of seven identical transformer chips before and after encapsulation. The peak values of the Q -factor show a negligible difference, however the difference was increased near the self-resonance frequency.

performance, seven identical chips were characterized, before and after the encapsulation. As a result of the increase in capacitance, the resonance frequency of the transformers was shifted on average from 312 to 256 MHz (figure 8).

However, we observed only a negligible change in the peak value of the quality factor and the power efficiency by the encapsulation (figures 9 and 10). Nevertheless, when approaching the self-resonance frequency, the quality factor of encapsulated chips was clearly lower than non-encapsulated chips.

According to the measurements, encapsulating the chips decreased the resonance frequency and also the quality factor near the resonance. However, both the quality factor and the power efficiency peak value were not affected by the encapsulation. Details of the measured values for the seven identical chips, before and after the packaging are summarized in the table 4.

3.4. Batch fabrication potential

The repeatability of the production process was further investigated, to demonstrate the eligibility of the process for batch fabrication. Twenty five transformers were sequentially wound on SU-8 posts, in a single process step, on a single wafer substrate. The devices were characterized to compare their main properties and to estimate the process repeatability. The transformers' designs were almost identical to those presented

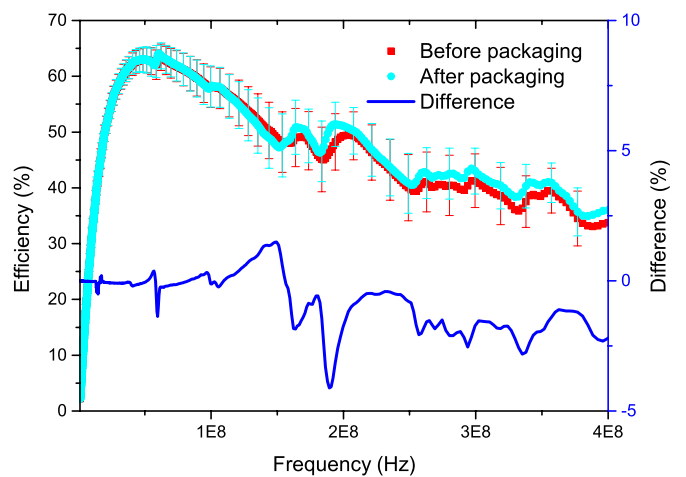


Figure 10. Measured power efficiency versus frequency of seven identical transformer chips. The peak values of the efficiency show a negligible difference, however the difference (thin blue line) was increased approaching the self-resonance frequency.

in section 2, but with 18 windings instead of 20. Figure 11 depicts the results from all 25 samples.

Standard deviations for the primary and the secondary inductances are 6.3 and 5 nH, for resistances the values are 0.032 and 0.040 Ω , for the quality factors the values are

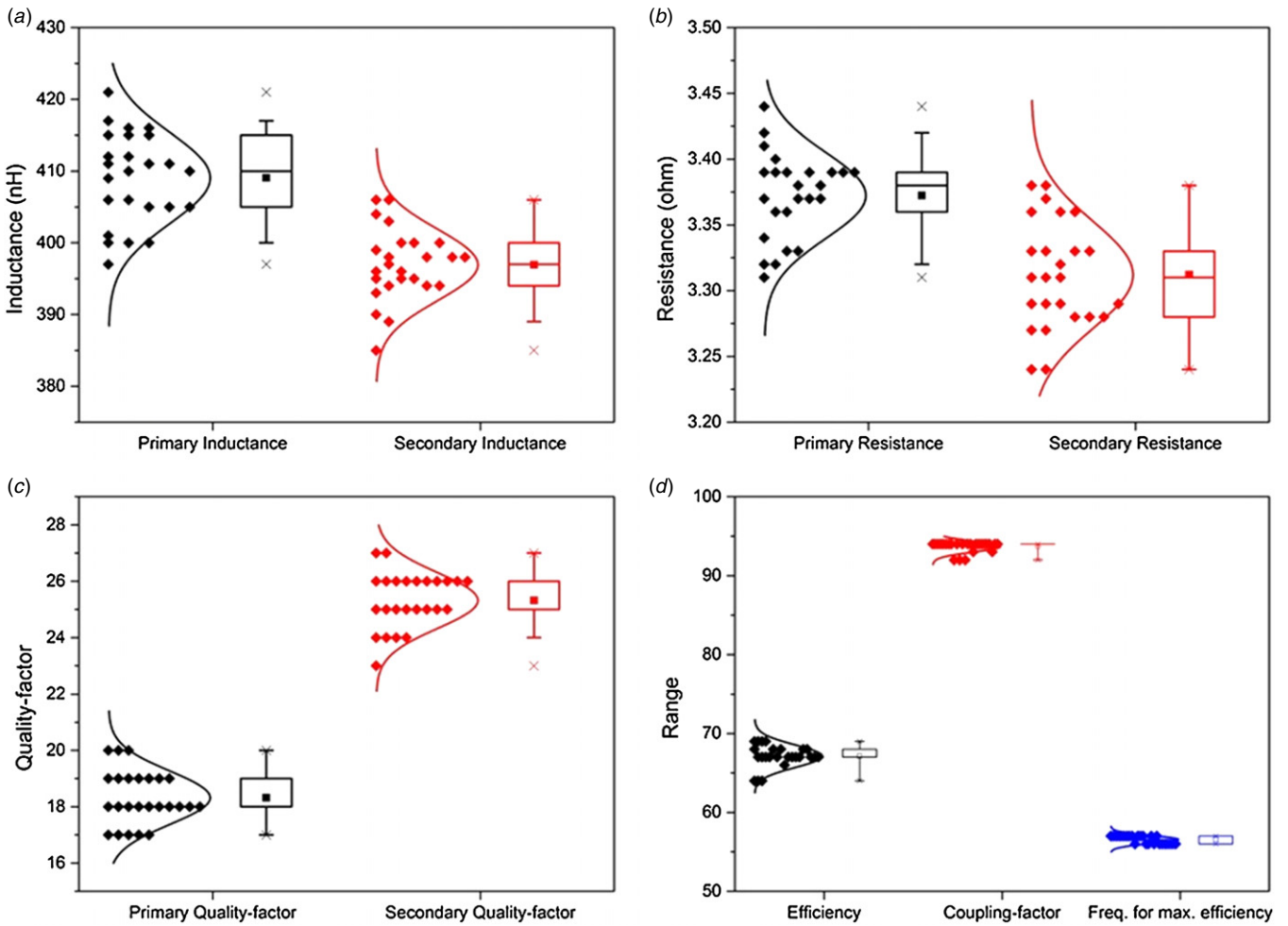


Figure 11. Process variations for 25 wire bonded transformers. The measured results demonstrate the suitability of wire bonded transformers for batch fabrication.

0.94 and 0.99, as well as for maximum efficiency we found 1.42%, for the coupling factor the value was 0.69%, and for the frequency corresponding to the maximum efficiency, the standard deviation was found to be 0.5 MHz.

4. Conclusion

We have demonstrated a fast, flexible and repeatable process for the fabrication of air core, on-chip microtransformers intended for VHF applications in the 30–300 MHz regime. For the fabrication of the primary and secondary coil windings, we used an automatic wire bonder, achieving a high manufacturing throughput, and at the same time improved the electrical performance with respect to previous reports.

We successfully introduced insulated copper wire to the coil winding process to replace the commonly used, yet more expensive, gold wire. Based on our results, copper wire has the advantage of decreasing a coil’s resistance for frequencies below 20 MHz for 25 μm thick wire. At higher frequencies, however, parasitic losses due to the skin and proximity effect become dominant, which offsets the enhanced conductivity of the copper, finally resulting in similar maximum quality factors for gold and copper coils. In order to use the copper wire

efficiently, a feedstock with higher wire diameter is needed to address copper’s RF skin depth at typical frequencies of interest.

Simulation models based on the wire bonding trajectories have been generated using the FastHenry software, in order to accurately predict and optimize a transformers’ properties prior to fabrication. The results achieved showed a good match between measured and simulated inductances, as well as the coupling factors. However, for the resistance calculations, the simulation error was unacceptable, probably due to a software limitation to rectangular wire cross-sections.

In order to protect coils from environmental factors and mechanical damage, the coils were encapsulated in PDMS. Experimental results indicated that the encapsulation approach did not compromise a transformer’s electrical performance.

The repeatability of the fabrication process based on wire bonding was investigated by comparing the measured electrical data of 25 identically processed devices. The low standard deviation of the results demonstrated the suitability of the process for batch fabrication.

To conclude this work, we benchmarked the microtransformers to previously published devices (but excluding pure RF transformers). Figure 12 plots the

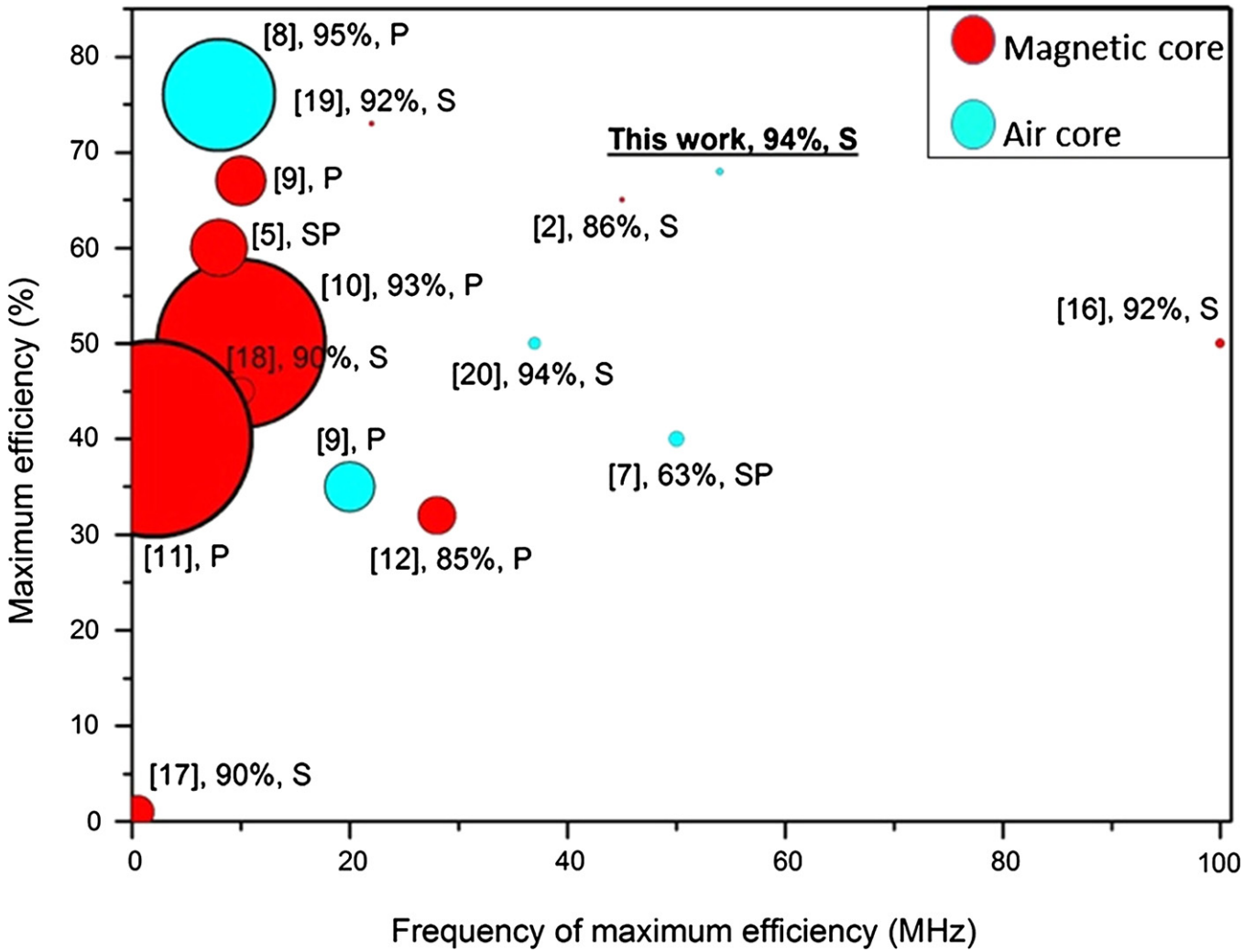


Figure 12. A comparison of published microtransformer characteristics (but excluding RF devices). Blue bubbles represent transformers with air core, red bubbles with magnetic core. The bubble size represents the device footprint. The labels indicate the reference numbers, the coupling factors, and whether the transformer coil designs are solenoidal (S), planar (P), or stacked planar (SP).

maximum device efficiency as a function of the frequency at which the maximum appeared. The size of the bubbles indicates the footprint area of each transformer, whereas the color of a bubble distinguishes between air core and magnetic-core transformers. The additional number represents the maximum coupling factor. The transformers presented in this paper, represented by a very small blue bubble, convinces through its small footprint, reasonably large frequency range, high efficiency and high coupling factor. Only two other microtransformers are comparable in footprint and performance, namely [19], however at lower frequency, and [16] at lower efficiency. In contrast to these two devices, the clear advantage of the present transformer is its air core. The complete avoidance of magnetic materials makes the resulting process straightforward, lean and absolutely CMOS compatible.

Already from the present point of view, our compact and extremely precise 3D coil winding procedure renders air core transformers competitive. Nevertheless, there is still space for improvement. An effective strategy to reduce the internal losses would be to increase the wire diameter and

hence its circumference, which would help in terms of the skin effect. Another measure would be to increase the pitch of windings in order to decrease the proximity effect. Both strategies will advance the transformers further towards an optimum efficiency for the VHF domain.

Our next research steps will be to evaluate our transformers for the DC–DC convertor application. This will help us to also qualify them with regard to their current/voltage capabilities as well as thermal characteristics.

Acknowledgments

This work was supported by the DFG graduate school *Embedded Microsystem* under grant number 1103. We are grateful to the laboratory of electrical instrumentation, especially to Jochen Hempel, for access to their HF characterization setup. We thank Kai Steffen for electroplating the bond pads and traces, Thilo Brunn for his help in characterization, and Jens Brunne for support in PDMS processing.

References

- [1] Park J Y and Allen M G 2003 Ultralow-profile micromachined power inductors with highly laminated Ni/Fe cores: application to low-megahertz DC-DC converters *IEEE Trans. Magn.* **39** 3184–6
- [2] Raimann M, Peter A, Mager D, Wallrabe U and Korvink J G 2012 Microtransformer-based isolated signal and power transmission *IEEE Trans. Power Electron.* **27** 3996–4004
- [3] Flynn D, Toon A, Allen L, Dhariwal R and Desmulliez M P Y 2007 Characterization of core materials for microscale magnetic components operating in the megahertz frequency range *IEEE Trans. Magn.* **43** 3171–80
- [4] O'Donnell T, Wang N, Meere R, Rhen F, Roy S, O'Sullivan D and O'Mathuna C 2008 Microfabricated inductors for 20 MHz Dc-Dc converters *IEEE, 2008: 23rd Annu. Applied Power Electronics Conf. and Exposition* pp 689–93
- [5] Sullivan C and Sanders S 1996 Design of microfabricated transformers and inductors for high-frequency power conversion *IEEE Trans. Power Electron.* **11** 228–38
- [6] Tang S, Hui S and Chung H 2001 A low-profile low-power converter with coreless PCB isolation transformer *IEEE Trans. Power Electron.* **16** 311–5
- [7] Yamaguchi K, Sugawara E, Nakajima O, Matsuki H and Murakami K 1993 Load characteristics of a spiral coil type thin film microtransformer *IEEE Trans. Magn.* **29** 3207–9
- [8] Mino M, Yachi T, Tago A, Yanagisawa K and Sakakibara K 1996 Planar microtransformer with monolithically-integrated rectifier diodes for micro-switching converters *IEEE Trans. Magn.* **32** 291–6
- [9] Brunet M, O'Donnell T C, Baud L, O'Brien J, McCloskey P and O'Mathuna S C 2002 Electrical performance of microtransformers for DC-DC converter applications *IEEE Trans. Magn.* **38** 3174–6
- [10] Park J Y and Bu J U 2003 Packaging compatible microtransformers on a silicon substrate *IEEE Trans. Adv. Packag.* **26** 160–4
- [11] Meyer C D, Bedair S S, Morgan B C and Arnold D P 2010 High-inductance-density, air-core, power inductors, and transformers designed for operation at 100–500 MHz *IEEE Trans. Magn.* **46** 2236–9
- [12] Sullivan C R and Sanders S R 1995 Microfabrication process for high-frequency power-conversion transformers *IEEE, Proc. PESC—Power Electronics Specialist Conf.* vol 2 pp 658–64
- [13] Ehrmann K, Saillen N, Vincent F, Stettler M, Jordan M, Wurm F M, Besse P-A and Popovic R 2007 Microfabricated solenoids and Helmholtz coils for NMR spectroscopy of mammalian cells *Lab Chip* **7** 373–80
- [14] Jackman R J, Rogers J A and Whitesides G M 1997 Fabrication and characterization of a concentric cylindrical microtransformer *IEEE Trans. Magn.* **33** 2501–3
- [15] Kurata H, Shirakawa K, Nakazima O and Murakami K 1994 Solenoid-type thin-film micro-transformer *IEEE Transl. J. Magn. Japan* **9** 90–4
- [16] Rassel R and Hiatt C 2003 Fabrication and characterization of a solenoid-type microtransformer *IEEE Trans. Magn.* **39** 553–8
- [17] Xu M and Liakopoulos T 1998 A microfabricated transformer for high-frequency power or signal conversion *IEEE Trans. Magn.* **34** 1369–71
- [18] Kratt K, Badilita V, Burger T, Korvink J G and Wallrabe U 2010 A fully MEMS-compatible process for 3D high aspect ratio micro coils obtained with an automatic wire bonder *J. Micromech. Microeng.* **20** 015021
- [19] Moazenzadeh A, Spengler N and Wallrabe U 2012 On-chip, MEMS-scale, high-performance, 3D-solenoidal transformers *12th Int. Workshop on Micro and Nanotechnology for Power Generation and Energy Conversion Applications (Atlanta)* pp 22–5
- [20] Moazenzadeh A, Spengler N and Wallrabe U 2013 High-performance, 3D-microtransformers on multilayered magnetic cores *IEEE, 26th Int. Conf. on Micro Electro Mechanical Systems (MEMS) (Taipei, 2013)* pp 287–90
- [21] Kamon M, Michael J and White J K 1994 FASTHENRY: a multipole-accelerated 3-D inductance extraction program *IEEE Trans. Microw. Theory Tech.* **42** 1750–8
- [22] Mathúna S and O'Donnell T 2005 Magnetics on silicon: an enabling technology for power supply on chip *IEEE Trans. Power Electron.* **20** 585–92
- [23] Wheeler H 1928 Simple inductance formulas for radio coils *Proc. Inst. Radio Eng.* **16** 1398–400
- [24] Pozar D M 2011 *Microwave Engineering, Fourth Edition* (Amherst, MA: Wiley)
- [25] Shah A, Mayer M, Zhou Y N, Hong S J and Moon J T 2009 Low-stress thermosonic copper ball bonding *IEEE Trans. Electron. Packag. Manuf.* **32** 176–84
- [26] Zhong Z W 2011 Overview of wire bonding using copper wire or insulated wire *Microelectron. Reliab.* **51** 4–12
- [27] www.dowcorning.com/applications/search/default.aspx?r=131en
- [28] Schneider F, Fellner T, Wilde J and Wallrabe U 2008 Mechanical properties of silicones for MEMS *J. Micromech. Microeng.* **18** 065008